

# Field-induced metal-insulator transition and switching phenomenon in correlated insulators

Naoyuki Sugimoto,<sup>1</sup> Shigeki Onoda,<sup>2</sup> and Naoto Nagaosa<sup>1,3</sup>

<sup>1</sup> *Department of Applied Physics, University of Tokyo, Tokyo 7-3-1, Hongo, Tokyo 113-8656, Japan\**

<sup>2</sup> *Condensed Matter Theory Laboratory, RIKEN (The Institute of Physical and Chemical Research), Wako 351-0198, Japan*

<sup>3</sup> *Cross-Correlated Materials Research Group (CMRG), ASI,*

*RIKEN, 2-1 Hirosawa, Wako, Saitama 351-0198, Japan*

(Dated: November 6, 2018)

We study the nonequilibrium switching phenomenon associated with the metal-insulator transition under electric field  $E$  in correlated insulator by a gauge-covariant Keldysh formalism. Due to the feedback effect of the resistive current  $I$ , this occurs as a first-order transition with a hysteresis of  $I$ - $V$  characteristics having a lower threshold electric field ( $\sim 10^4 \text{Vcm}^{-1}$ ) much weaker than that for the Zener breakdown. It is also found that the localized mid-gap states introduced by impurities and defects act as hot spots across which the resonant tunneling occurs selectively, which leads to the conductive filamentary paths and reduces the energy cost of the switching function.

PACS numbers: 71.30.+h, 72.20.Ht, 72.10.Bg

In correlated electronic systems, the Coulomb interaction and the electron-phonon coupling give rise to various long-range orderings of spin, charge, and orbital degrees of freedom of electrons, providing rich phase diagrams and intriguing phenomena such as colossal magnetoresistance [1]. The collective response can be significantly sensitive and amplified in comparison with that in semiconductors [2], because many electrons cooperate in a short length scale of nanometres owing to the high electron density. These orderings often lead to an insulating behavior with an energy gap in the single-electron spectrum represented by the Mott gap [3]. In sharp contrast to the band insulators, the gap itself can be controlled by the external stimuli, as observed in experiments on the metal-insulator transition driven by the electric field [4, 5] or the light irradiation [6, 7]. Furthermore, metal-insulator switching phenomena have been observed in other correlated electronic systems such as organic charge-transfer compounds [8],  $\text{La}_{2-x}\text{Sr}_x\text{NiO}_4$  [9], one-dimensional Mott insulators  $\text{Sr}_2\text{CuO}_3/\text{SrCuO}_2$  [10]. Recently, the application of the switching phenomenon to electronic devices has also been seriously considered [11]. One important observation here is that the threshold electric fields observed in the correlated systems are typically  $10^4 \text{V/cm}$  [9, 10] which is much less than  $\sim 10^6 \text{V/cm}$  expected from the simple Zener breakdown (see below). This suggests a positive feedback effect of the collective nature of the metal-insulator transition in the switching phenomena. Also the current is often non-uniform and confined in narrow paths or filaments [5, 12].

Theoretically, on the other hand, the description of the nonequilibrium states still remain a challenge even though there are several related works [13, 14, 15]. Especially the non-perturbative treatment of the steady state under a strong electric field has been a difficulty. Re-

cently, we have developed such formalism to deal with the far-from-equilibrium states [16]. This enables us to exactly incorporate the effects of the electric field into the Dyson equation for the nonequilibrium Green's function, which is written in a compact form by using the Moyal product in the gauge-covariant Wigner representation.

In this Letter, we develop a theory of resistive switching phenomenon in the spin/charge ordered correlated insulators employing the gauge-covariant Keldysh formalism combined with the mean-field approximation to the electron-electron interaction. Then, the hysteric resistive switching due to the applied electric field has been obtained theoretically for the first time as far as we know. The theory also accounts the experimentally observed low threshold field and filament formation.

We study the one-dimensional interacting electrons described by

$$\hat{H} = \sum_{p\sigma} \varepsilon(p) c_{p,\sigma}^\dagger c_{p,\sigma} + g \sum_{p_1, p_2, q} c_{p_1+q, \uparrow}^\dagger c_{p_2-q, \downarrow}^\dagger c_{p_2, \downarrow} c_{p_1, \uparrow}, \quad (1)$$

where  $g$  is assumed to be a constant and repulsive and the other notations are standard. This interaction naturally leads to the spin density wave ordering at the wavevector  $2k_F$  ( $k_F$ : Fermi wavenumber), which is assumed to be half of the reciprocal lattice vector  $G$ , i.e., half-filling, and introduces the gap  $2\Delta$ . The sign of the gap is the opposite for the opposite spin, and we can just consider the two copies of the spinless electrons by the mean field Hamiltonian;

$$\hat{H} \cong \sum_p \vec{c}_p^\dagger \begin{pmatrix} vp & \Delta \\ \Delta & -vp \end{pmatrix} \vec{c}_p, \quad (2)$$

where,  $\vec{c}_p = {}^t(c_{p,R}, c_{p,L})$  is the two component operator corresponding to the right-going and left-going electrons near  $\pm k_F$  with the dispersion  $\pm vp$  ( $v$ : velocity). Here,  $2\Delta := g \langle c_{p,R}^\dagger c_{p,L} \rangle$  is the self-consistently determined gap (see Eq. (4)). While this ordered state in equilibrium

\*Electronic address: sugimoto@appi.t.u-tokyo.ac.jp

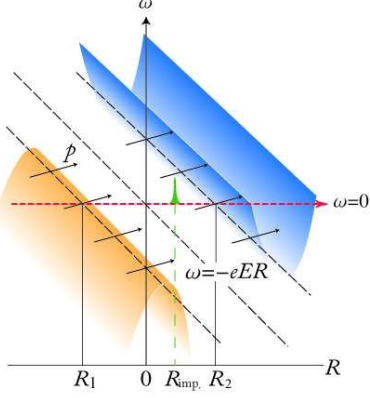


FIG. 1: The tilted band structure under an external electric field  $E$ . At each spatial position  $R$ , the momentum  $p$  is defined as shown in the orthogonal direction. The conduction band bottom and the valence band top cross the energy  $\omega = 0$  at  $R_2$  and  $R_1$ , respectively. The localized impurity state at  $R = R_{\text{imp}}$  with green color gives rise to the resonant tunneling.

is well-known, we are interested in the nonequilibrium phase transition driven by the electric field. Note that the ordering is commensurate, and the phason degrees of freedom is quenched in sharp contrast to the sliding charge density wave problem [17]. The interaction is treated in the mean-field approximation, which is justified in the weak to intermediate-coupling regime, though a more elaborate treatment is required in the strong-coupling regime.

We separate the problem into two steps, i.e., (i) to describe the current flowing state under the electric field in the mean field Hamiltonian Eq. (2), and (ii) to solve the self-consistent equation  $2\Delta = g\langle c_{p,R}^\dagger c_{p,L} \rangle$  for the gap. The first step is basically the Zener tunneling problem studied previously [18, 19, 20, 21, 22, 23]. As schematically shown in Fig. 1, the electrons tunnel through the energy gap. The band structure is spatially tilted by the potential energy gain  $-eER$  where  $R$  is the real space position and  $-e$  is the electronic charge. One can consider the locally defined band structure as a function of the momentum (which is represented along the transverse axis) at each  $R$ , and the equi-energy line crosses the bottom (top) of the conduction (valence) band at  $R = R_1$  ( $R = R_2$ ). The wavefunctions of conduction and valence bands tunnel through the potential barrier between  $R_1$  and  $R_2$  from the both sides.

There are three length scales with this problem; (i) the correlation length  $\zeta = \hbar v / 2\Delta$  associated with the energy gap  $2\Delta$ , which describes the characteristic extent of the wave packet relevant to the tunneling, (ii) the tunneling length  $\xi = 2\Delta / eE = R_2 - R_1$  over which an electron can gain the energy  $2\Delta$  by the electric field  $E$ , and (iii) the mean free path  $\ell$ . The Zener tunneling occurs quite differently depending on the relative magnitudes of these length scales. We will focus below the case of  $\ell \gg \zeta$ ;

the mean free path is much longer than the correlation length, or the energy gap  $2\Delta$  is much larger than the energy broadening  $\hbar v / \ell$  due to the impurity scatterings. Then the Zener tunneling is controlled by the ratio of  $\xi / \zeta$ . When  $\xi \gg \zeta$ , the Zener tunneling probability can be calculated in the semi-classical approximation as  $\sim \exp[-\pi\xi / 2\zeta]$  [23]. As we increase the electric field so that  $\xi < \zeta$ , the wave packet extends from  $R_1$  to  $R_2$  and the metallic conduction occurs, i.e., the crossover between the Zener tunneling and Ohmic regions.

Although this picture is valid qualitatively, it is crucial to consider steady state with the dissipative current flowing to describe the nonequilibrium phase transition. We perform the self-consistent calculations of Green's functions and self-energies in the Keldysh space in the gauge-covariant Wigner representation, which is now composed of the mechanical energy and momentum [16, 24]. It is necessary to introduce the Green's functions and the self-energies in the Keldysh space,  $\underline{G} := \begin{pmatrix} \hat{G}^R & 2\hat{G}^< \\ 0 & \hat{G}^A \end{pmatrix}$ , and  $\underline{\Sigma} := \begin{pmatrix} \hat{\Sigma}^R & 2\hat{\Sigma}^< \\ 0 & \hat{\Sigma}^A \end{pmatrix}$ , respectively [16]. Kinetic equations of the functions are given in the form of the Dyson equations:  $(\hat{\mathcal{L}} - \underline{\Sigma}) \star \underline{G} = 1$  and  $\underline{G} \star (\hat{\mathcal{L}} - \underline{\Sigma}) = 1$  with  $\hat{\mathcal{L}}(\omega, p) := \omega - \hat{H}(p)$ . The symbol  $\star$  denotes the Moyal product:  $(f \star g)(x) = \frac{1}{(\pi e \hbar v)^2} \int dy dz f(y) g(z) e^{-\frac{2i}{e \hbar v} ((x^\mu - y^\mu) S_{\mu\nu} (x^\nu - z^\nu))}$ , where  $x, y, z$  denote the two-dimensional energy-momentum coordinates  $(\omega, vp)$ ,  $f$  and  $g$  are the smooth functions of the energy-momentum, and  $S_{\mu\nu} := \begin{pmatrix} 0 & -1 \\ 1 & 0 \end{pmatrix}$ .

Now, we turn to the calculation of  $\hat{G}^{R,A}$  and  $\hat{G}^<$  for the Landau-Zener model with the  $\delta$ -functional random impurity potential. Let us start with the pure case of  $\hat{\Sigma}^{R,A} = \mp i\eta$  with an infinitesimal number  $\eta$ . By using a Fourier transform:  $\mathcal{F}[f](\omega, \epsilon) := \int \frac{dp}{2\pi\hbar} f(\omega, p) e^{-2i p \epsilon / \hbar e E}$ , we obtain the Green's function in the pure case as

$$\hat{G}_{\text{pure}}^{R,A}(\omega, p) = \sum_{s=1,2} \frac{2}{eE} \int d\epsilon d\Upsilon \frac{\hat{\Phi}_s(\Upsilon + \epsilon) \hat{\Phi}_s^\dagger(\Upsilon - \epsilon)}{\omega - \Upsilon \pm i\eta} e^{\frac{2i p \epsilon}{e \hbar E}}, \quad (3)$$

where  $\hat{\Phi}_s := {}^t (\Phi_s^+, \Phi_s^-)$  are the solutions of the following Weber equations [19]:  $(\partial_z^2 + \frac{1}{2} \pm i \frac{\Delta^2}{2e\hbar v} - \frac{z^2}{4}) \Phi_s^\pm \left( \sqrt{\frac{eE\hbar v}{2}} e^{\mp \frac{i\pi}{4}} z \right) = 0$  with a normalization condition:  $\sum_{s=1,2} \int d\lambda \hat{\Phi}(\lambda - \omega) \hat{\Phi}^\dagger(\lambda - \omega') = \delta((\omega - \omega') / eE)$ . We employed the self-consistent Born approximation;  $\hat{\Sigma}^{R,A}(\omega) = n_i u^2 \hat{g}^{R,A}(\omega, \epsilon = 0)$ , with the density of impurities  $n_i$  and the strength of the potential  $u$  leading to the lifetime  $\tau := (v\hbar^2 / n_i u^2)$  and the mean-free path  $\ell := \tau v$ . Then, we calculate the retarded and advanced Green's functions through  $\hat{G}^{R,A} = \hat{G}_{\text{pure}}^{R,A} + \hat{G}_{\text{pure}}^{R,A} \star \hat{\Sigma}^{R,A} \star \hat{G}^{R,A}$ . Finally, the lesser Green's function is obtained as  $\hat{G}^< \cong f_F \star \hat{G}^A - \hat{G}^R \star f_F + \hat{G}^R \star [f_F \star \hat{\mathcal{L}}] \star \hat{G}^A$  with the Fermi distribution function  $f_F(\omega)$ . Here, we ne-

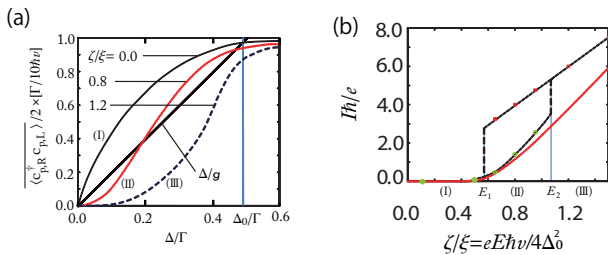


FIG. 2: (a): The right-hand side of the gap equation Eq. (4),  $\langle c_{p,R}^\dagger c_{p,L} \rangle / 2$  in the unit of  $(\Gamma/10\hbar v)$  as a function of the gap  $\Delta$  for  $\zeta/\xi = eE\hbar v/4\Delta_0^2 = 0.0, 0.8, 1.2$ , with  $\Gamma$  being the energy cutoff, i.e., the half bandwidth of the equilibrium states. Here,  $\Delta_0$  is the gap in the equilibrium for  $g = 5\hbar v$ . The solid straight line represents  $\Delta/g$  in the same unit and the crossing of these two gives the solution(s) to the mean field equation (4). (b): The obtained current  $I$  as a function of the electric field  $E$ . The dashed line is a guide to the eyes. The  $I$ - $E$  characteristics clearly shows the hysteresis and switching behavior of the current. The red dotted curve represents the current obtained for the fixed gap  $\Delta_0$ .

glect a vertex correction since it gives only a minor correction [25].

The self-consistent mean-field gap equation of  $\Delta$  for a given interaction strength  $g$  is given by

$$\frac{1}{g}\Delta = \overline{\langle c_{p,R}^\dagger c_{p,L} \rangle} / 2 \equiv \int \frac{d\omega}{4i\pi} \frac{dp}{2\pi\hbar} \text{tr} \left[ \hat{\sigma}^x \hat{G}^<(\omega, p) \right], \quad (4)$$

the right-hand side of which is a function of the electric field  $E$  and the gap  $\Delta$  itself. Throughout this paper, we take  $g = 5\hbar v$ . The solution is obtained by the crossings of the straight line  $\Delta/g$  and the curve for  $\overline{\langle c_{p,R}^\dagger c_{p,L} \rangle} / 2$  in Fig. 2(a). There exist three regions of the strength of the electric field as (I)  $E < E_1$ , (II)  $E_1 < E < E_2$ , and (III)  $E > E_2$ , where the number of solutions to Eq. (4) is two, three, and one, respectively. Note that the stability of each solution is determined by the condition  $\partial \left( \overline{\langle c_{p,R}^\dagger c_{p,L} \rangle} / 2 \right) / \partial \Delta < 1/g$ . Thus, in region (I), the finite- $\Delta$  solution is the only stable one. In Fig. 2(a), we show the case of the equilibrium ( $E = 0$ ) with the gap  $\Delta_0$ . In the region (II), there are two stable solutions, i.e.,  $\Delta = 0$  and  $\Delta \neq 0$  as shown for the case of  $\zeta/\xi = eE\hbar v/4\Delta_0^2 = 0.8$  in Fig. 2(a), except the intermediate unstable one. This is the typical situation of the first-order phase transition. In the region (III), the stability of the  $\Delta \neq 0$  solution is lost, and the metallic state ( $\Delta = 0$ ) becomes the only stable solution, as shown for the case of  $\zeta/\xi = 1.2$  in Fig. 2(a). Therefore, we conclude that the spin/charge ordered system shows the first-order-like switching phenomenon.

We argue that these two threshold electric fields are essentially given by  $E_1 = \Delta_0/e\hbar v\tau$  and  $E_2 = \Delta_0^2/e\hbar v$ . It is easy to understand that  $E_2$  is the Zener breakdown field since at  $E > E_2$ , the gap does not prevent the metal-

lic current flow and hence the insulating state is unstable. To understand why the lower threshold field  $E_1$  appears, it is useful to consider the instability of the metallic current-carrying state. The steady state with the current is characterized by the shift of the electron distribution function by the amount  $\delta k = eE\tau$  with  $\tau = \ell/v$  being the mean-free time. With this shift, the energy difference between the right and left-moving electrons at the shifted Fermi level is  $\delta\varepsilon = 2v\delta k$ . When this energy is larger than the gap  $2\Delta_0$  in the equilibrium state, the instability toward the SDW/CDW disappears. This consideration leads to the estimation  $E_1 = \Delta_0/e\hbar v\tau$ , which is smaller than the Zener breakdown field  $E_2 = \Delta_0^2/e\hbar v$  by the factor  $\hbar/(\tau\Delta_0) \ll 1$ .

Now we study the physical properties associated with the switching phenomenon. Of the most important is the  $I$ - $E$  characteristics. The current  $I$  flowing through the sample is obtained from the relation

$$I = \frac{e^2 v^2 E}{2} \int \frac{d\omega}{2\pi} \frac{dp}{2\pi} \text{tr} \left[ \hat{\sigma}^z \hat{G}^R \star \left( -\hat{\sigma}^z \frac{\partial f_F}{\partial \omega} \right) \star \hat{G}^A \right]. \quad (5)$$

Figure 2(b) shows the  $I$ - $E$  characteristics corresponding to the first-order phase transition of the order parameter obtained in Fig. 2(a). There occurs the jump of the current, the upper branch of which corresponds to the metallic conduction while the lower branch to the Zener tunneling in the insulating state. The two threshold electric fields  $E_1$  and  $E_2$  can be separated by a factor as discussed above, and the change of the current is by the factor of  $\sim \exp(4\Delta^2/e\hbar vE)$ .

We also propose the measurement of the local density of states (LDOS) in terms of the scanning tunneling spectroscopy (STS) to study the nonequilibrium state. Based on the formula for the tunneling current given by Meir and Wingreen [26], we have calculated the STS LDOS as shown in Fig. 3. There appears a peak at the middle of the gap whose height is proportional to the tunneling current. Namely, the tunneling occurs through the in-gap density of states induced by the electric field. In the metallic state after the switching, of course the gap completely closes.

Now the semi-quantitative estimation for the realistic situation is in order. Typically,  $2\Delta$  is of the order of  $1eV$ , while  $\hbar/\tau$  is  $\sim 10meV$ , which leads to the factor of  $\sim 100$  reduction of the switching threshold from the Zener breakdown field  $\sim 10^6V/cm$ . Therefore, the observed values of the order of  $10^4V/cm$ [9, 10] is in the reasonable range as expected from the present consideration. A threshold current density  $j_1$  is estimated by  $j_1 \sim (\Delta n a)(e/\hbar)$ , where  $n$  denotes a density of the electron. By using the typical values, we estimate the current density as  $j_1 \sim 10^8 A/cm^2$ . This is a very large current density, and can be usually realized only in the pulse current experiment since the huge heat generation makes the sample burned out.

However, the breakdown and switching occur often in the filamentary paths of metallic regions [5, 12]. As mentioned above, the emerging in-gap state is associ-

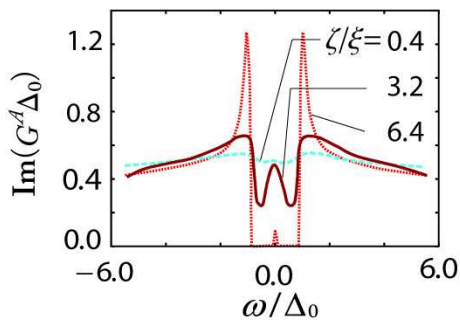


FIG. 3: The local density of states (LDOS)  $\text{Im}(\hat{G}^A \Delta_0)$  as a function of the normalized energy  $\omega/\Delta_0$  ( $\Delta_0$ : the energy gap in the equilibrium) for  $\zeta/\xi=6.4$  (dashed line), 3.2 (solid line) and 0.4 (dotted line), respectively. ( $\zeta = \hbar v/2\Delta_0$ : correlation length,  $\xi = 2\Delta_0/eE$ )

ated with the tunneling. In real materials, there are often in-gap states due to the impurities, vacancies, *etc* even without the electric field. Suppose there is an impurity level in the gap as shown by the green peak at  $R = R_{\text{imp}}$ . in Fig. 1. Let  $t_1$  be the tunneling amplitude from the valence band at  $R = R_1$  to the impurity level, while  $t_2$  be that from there to the conduction band at  $R = R_2$ . Note that  $t_1$  and  $t_2$  are exponentially small, i.e.,  $t_1 \sim \exp(-\pi(R_{\text{imp.}} - R_1)/2\zeta)$ ,  $t_2 \sim \exp(-\pi(R_2 - R_{\text{imp.}})/2\zeta) \ll 1$ , with the product  $t_1 t_2$  being the Zener tunneling amplitude without the resonant level. Considering the two barrier problem with the small tunneling amplitudes of  $t_1$  and  $t_2$ , the tunneling probability through the two barriers has the peak height given by  $T_{\text{max}} \cong [2t_1 t_2 / (t_1^2 + t_2^2)]^2$  within the narrow energy width  $\delta\varepsilon \cong W(t_1^2 + t_2^2)$ , which can be translated into the width in the real-space  $\delta R \cong \delta\varepsilon/(eE)$  in Fig.1. When the extent of the electron wave packet is larger than  $\delta R$  (which is the case in the limit of small tunneling amplitude), the averaged tunneling probability is of the order of  $t_1^2 t_2^2 / (t_1^2 + t_2^2)$ . This is much larger than that without the impurity level, i.e.,  $(t_1 t_2)^2$  corresponding to the tunneling amplitude  $t_1 t_2$  for the Zener tunneling. This means that there appear “hot spots” at  $R_1$  and  $R_2$  which are spatially separated by  $\zeta$ . Therefore the impurities act as the nucleation centers of the

nonequilibrium first-order metal-insulator phase transition discussed above. With the random configuration of the impurities, the current can find the path along where this nucleation centers populate densely compared with the other spatial region. This leads to the filamentary paths of the metallic regions as observed experimentally.

Since the width of the filamentary path is given by the correlation length  $\zeta$ , which characterizes also the spatial variation of the SDW/CDW order parameter, a threshold current  $I_1$  is estimated by  $I_1 \sim \pi\zeta^2 \cdot j_1 = (nav^2/\Delta)(\pi e\hbar) \sim 1\mu\text{A}$ . From this expression, we found that the switching occurs with rather tiny current in correlated insulators. Moreover, from a point of view of the Joule heating, the correlated insulator is more advantageous over semiconductors. The Joule heat corresponding to the breakdown is written as  $P = j_1 \cdot E_1 = (\Delta a)^2(1/\hbar v\tau)$ . For the correlated insulator, this is estimated as  $P_{\text{cor.}} \sim 10^{12}\text{VA/cm}^3$ . This value is rather similar to that in the typical semiconductors. However, as mentioned above, the current is confined within filaments of nano-scale in the correlated systems, while it is rather uniformly distributed in semiconductors. Therefore, the total heat generation  $P'_{\text{cor.}}$  is expected to be much smaller in correlated insulator as  $P'_{\text{cor.}} = \varrho\pi\zeta^2 j \sim \varrho \times 10^{-2}\text{VA/cm}^3$ , where  $\varrho$  denotes a density of the filaments. Once some filaments appear, the voltage drop across the sample disappears and no additional filaments are needed.

To summarize, we have studied the switching phenomenon of the correlated insulator under an applied electric field. Due to the feedback effect of the current on the spin/charge ordering, the switching occurs with much weaker field/smaller current/ smaller heat generation as compared with those expected from the simple Zener breakdown picture. This finding will be useful for the future application of this phenomenon to memory and switching devices.

S. O. thanks S. Okamoto for discussion. The work was partly supported by Grant-in-Aids (No. 15104006, No. 16076205, No. 17105002, No. 19048015) and NAREGI Nanoscience Project from the Ministry of Education, Culture, Sport, Science and Technology. S. O. was supported by Grant-in-Aids (No. 19840053) from Japan Society of the Promotion of Science.

- 
- [1] *Colossal magnetoresistive Oxides, Advances in Condensed Matter Science Vol. 2*, edited by Y. Tokura Gordon and Breach, Amsterdam, 2000.
- [2] S. M. Sze and K. Ng. Kwok, *Physics of Semiconductor Devices, Third edition*, John Wiley & Sons, Inc. 2007.
- [3] N. F. Mott, *Metal-Insulator Transitions* Taylor and Francis, London/Philadelphia, 1990.
- [4] A. Asamitsu, Y. Tomioka, H. Kuwahara and Y. Tokura, *Nature* **388**, 50 (1997).
- [5] N. Takubo, and K. Miyano, *Phys. Rev. B* **76**, 184445 (2007).
- [6] K. Miyano, T. Tonogai, T. Satoh, H. Oshima, and Y. Tokura, *Journal de Physique IV (Colloques)* **9**, 311-314 (1999).
- [7] K. Miyano, T. Tanaka, Y. Tomioka and Y. Tokura, *Phys. Rev. Lett.* **78**, 4257 (1997).
- [8] R. Kumai, Y. Okimoto and Y. Tokura, *Science* **284**, 1645-1647 (1999).
- [9] S. Yamanouchi, Y. Taguchi and Y. Tokura, *Phys. Rev. Lett.* **83**, 5555-5558 (1999).

- [10] Y. Taguchi, T. Matsumoto and Y. Tokura, Phys. Rev. B **62**, 7015 -7018 (2000).
- [11] A. Sawa, T. Fujii, K. Kawasaki and Y. Tokura, Appl. Phys. Lett. **85**, 4073 -4075 (2004).
- [12] J. Burgy, E. Dagotto and M. Mayr, Phys. Rev. B **67**, 014410 (2003).
- [13] Takashi Oka and Hideo Aoki, Phys. Rev. Lett. **95**, 137601 (2005) and references therein.
- [14] S. Okamoto and A. J. Millis, Nature (London) **428**, 630 (2004), and refences therein.
- [15] S. Okamoto, Phys. Rev. B **76**, 035105 (2007).
- [16] S. Onoda, N. Sugimoto, and N. Nagaosa, Prog. Theor. Phys. **116**, 61-86 (2006).
- [17] G. Gruner, *Density waves in solids*, Cambridge, Mass. Advanced Book Program : Perseus Publishing, 2000.
- [18] L. D. Landau, Phys. Zts. Sov. **2**, 46 (1932).
- [19] C. Zener, Proc. Roy. Soc. **A137**, 696 (1932).
- [20] E. C. G. Stueckelberg, Hel. Phys. Acta. **5**, 369 (1932).
- [21] Y. Gefen, E. Ben-Jacob and A. O. Caldeira, Phys. Rev. B **36**, 2770 (1987).
- [22] P. Ao and J. Rammer, Phys. Rev. B **43**, 5397 (1991).
- [23] J. M. Ziman, *Principles of the Theory of Solids*, Cambridge University Press, 1972, pp. 190.
- [24] N. Sugimoto, S. Onoda, and N. Nagaosa, Prog. Theor. Phys. **117**, 415-429 (2007).
- [25] G. Rikayzen, *Green's functions and condensed matter*, London ; Tokyo : Academic Press, 1980, pp. 109-119.
- [26] Y. Meir, and N. S. Wingreen, Phys. Rev. Lett. **68**, 2512 (1992).